



SUBJECT AREAS:  
SURFACE PATTERNING  
QUANTUM CHEMISTRY  
NANOPARTICLES  
MATERIALS CHEMISTRY

Received  
18 September 2012

Accepted  
5 November 2012

Published  
4 December 2012

Correspondence and requests for materials should be addressed to T.H. (t.heine@jacobs-university.de) or C.W. (christof.woell@kit.edu)

# A novel series of isorecticular metal organic frameworks: realizing metastable structures by liquid phase epitaxy

Jinxuan Liu<sup>1</sup>, Binit Lukose<sup>2</sup>, Osama Shekha<sup>1,3</sup>, Hasan Kemal Arslan<sup>1</sup>, Peter Weidler<sup>1</sup>, Hartmut Gliemann<sup>1</sup>, Stefan Bräse<sup>4,5</sup>, Sylvain Grosjean<sup>4,5</sup>, Adelheid Godt<sup>6</sup>, Xinliang Feng<sup>7</sup>, Klaus Müllen<sup>7</sup>, Ioan-Bogdan Magdau<sup>1,2</sup>, Thomas Heine<sup>2</sup> & Christof Wöll<sup>1</sup>

<sup>1</sup>Institute of Functional Interfaces, Karlsruhe Institute of Technology, 76344 Eggenstein-Leopoldshafen, Germany, <sup>2</sup>School of Engineering and Science, Jacobs University Bremen, 28759 Bremen, Germany, <sup>3</sup>Advanced Membranes & Porous Materials Center, King Abdullah University of Science and Technology, Thuwal, 23955-6900, Kingdom of Saudi Arabia, <sup>4</sup>Institute of Organic Chemistry, Karlsruhe Institute of Technology, 76131 Karlsruhe, Germany, <sup>5</sup>Soft Matter Synthesis Lab, Institute for Biological Interfaces, Karlsruhe Institute of Technology, 76344 Eggenstein-Leopoldshafen, Germany, <sup>6</sup>Department of Chemistry, Bielefeld University, 33615 Bielefeld, Germany, <sup>7</sup>Max-Planck-Institut für Polymerforschung, Ackermannweg 10, 55128, Mainz, Germany.

**A novel class of metal organic frameworks (MOFs) has been synthesized from Cu-acetate and dicarboxylic acids using liquid phase epitaxy. The SURMOF-2 isorecticular series exhibits P4 symmetry, for the longest linker a channel-size of  $3 \times 3 \text{ nm}^2$  is obtained, one of the largest values reported for any MOF so far. High quality, ab-initio electronic structure calculations confirm the stability of a regular packing of  $(\text{Cu}^{++})_2$ -carboxylate paddle-wheel planes with P4 symmetry and reveal, that the SURMOF-2 structures are in fact metastable, with a fairly large activation barrier for the transition to the bulk MOF-2 structures exhibiting a lower, twofold (P2 or C2) symmetry. The theoretical calculations also allow identifying the mechanism for the low-temperature epitaxial growth process and to explain, why a synthesis of this highly interesting, new class of high-symmetry, metastable MOFs is not possible using the conventional solvothermal process.**

Highly crystalline molecular scaffolds with nm-sized pores offer an attractive basis for the fabrication of novel materials. The scaffolds alone already exhibit attractive properties, e.g., the safe storage of small molecules like  $\text{H}_2$ ,  $\text{CO}_2$  and  $\text{CH}_4$ <sup>1</sup>. In addition to the simple release of stored particles, changes in the optical and electronic properties of these nanomaterials upon loading their porous systems with guest molecules offer interesting applications, e.g., for sensors<sup>2</sup> or electrochemistry<sup>3</sup>. For the construction of new nanomaterials, the voids within the framework of nanostructures may be loaded with nm-sized objects, such as inorganic clusters, larger molecules, and even small proteins<sup>4</sup>, a process that holds great potential, as, for example, in drug release<sup>5</sup> or the design of novel battery materials<sup>6</sup>. Furthermore, meta-crystals may be prepared by loading metal nanoparticles into the pores of a three-dimensional scaffold to provide materials with a number of attractive applications ranging from plasmonics<sup>7-9</sup> to fundamental investigations of the electronic structure and transport properties of the meta-crystals<sup>10</sup>.

In the last two decades, numerous studies have shown that MOFs, also termed porous coordination polymers (PCPs), fulfill many of the aforementioned criteria. Although originally developed for the storage of hydrogen, e.g., in tanks of automobiles, MOFs have recently found more technologically advanced applications as sensors<sup>2</sup>, matrices for drug release<sup>5</sup>, as membranes for enantiomer separation<sup>11</sup> and for proton conductance in fuel cells<sup>12</sup>. Although pore-sizes available within MOFs<sup>13</sup> are already sufficiently large to host metal-nanoclusters such as  $\text{Au}_{55}$ <sup>14,15</sup>, the actual realization of meta-crystals requires, in addition to structural requirements, a strategy for the controlled loading of the nanoparticles (NPs) into the molecular framework. Simply adding NPs to the solutions before starting the solvothermal synthesis of MOFs has been reported<sup>16</sup>, as well as the controlled encapsulation of nanoparticles<sup>17</sup>, but these procedures do not allow for the fabrication of nanoparticle superlattices with translational order. The layer-by-layer growing process of SURMOFs allows the uptake of nanosized objects during synthesis, including the fabrication of compositional gradients of different NPs<sup>18</sup>. Pure metal,

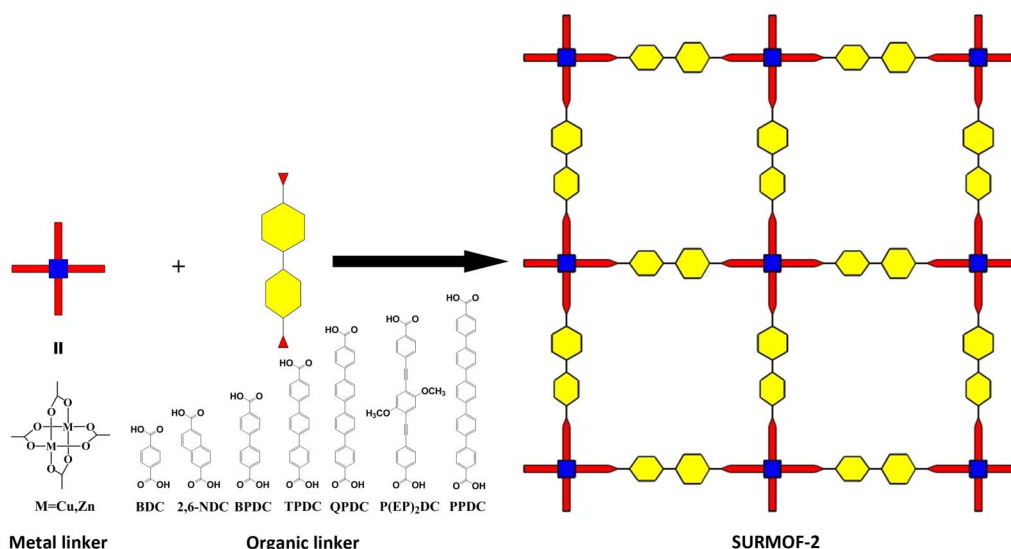


**Figure 1** | Schematic representation of the synthesis and formation of the SURMOF-2 analogues.

metal oxide or covalent cluster NPs have already been proposed for the fabrication of novel electronic devices<sup>10</sup>, but one may speculate that also the embedding of larger one-dimensional objects such as nanowires, carbon or inorganic nanotubes will be of interest.

The introduction of procedures for epitaxial growth of MOFs on functionalized substrates<sup>19</sup> was a major step towards controlled functionalization of frameworks. This liquid phase epitaxy (LPE) process allowed the preparation of compositional gradients<sup>20,21</sup> and provided a new strategy to load nano-objects into predefined pores.

Unfortunately, the LPE process has so far been only demonstrated for a fairly small number of MOFs<sup>11,19,22,23</sup>, none of which exhibits the required pore sizes. In addition, for the fabrication of meta-crystals, the architecture of the network should be sufficiently adjustable to realize pores of different sizes. There should also be a straightforward way to functionalize the framework itself in order to tailor the interaction of the walls with the targeted guest objects. Ideally, such a strategy would be based on an isorecticular series of MOFs in which the pore size can be determined by a choice from a homologous series of ligands with different lengths<sup>13</sup>.

Here, we present a novel isorecticular MOF series with the required flexibility as regards pore-sizes and functionalization, which is well suited for the LPE process. This class, denoted as SURMOF-2, is derived from MOF-2, one of the simplest framework architectures<sup>24,25</sup>. MOF-2 is based on paddle-wheel (pw) units formed by attaching 4 dicarboxylate groups to  $\text{Cu}^{2+}$  or  $\text{Zn}^{2+}$ -dimers, yielding planar sheets with 4-fold symmetry (see Fig. 1). These planes are held together by strong carboxylate/metal-bonds<sup>26</sup>. Conventional solvothermal synthesis yields stacks of pw-planes shifted relative to each other, with a corresponding reduction in symmetry to yield a P2 or C2 structure<sup>24,27,28</sup>.

## Results

**Experiments.** The relative shifts between the pw-planes can be avoided when using the recently developed liquid phase epitaxy (LPE) method<sup>22</sup>. As demonstrated by the XRD-data shown in Fig. 2, for a number of different dicarboxylic acid ligands, the LPE-process yields surface attached metal organic frameworks (SURMOFs) with P4 symmetry<sup>29</sup>, except for the 2,6-NDC ligand, which exhibits a P2 symmetry as a result of the non-linearity of the carboxyl functional groups on the ligand. Solvothermal synthesis conditions using either DMF or ethanol as solvent yield bulk MOF powder, which does not exhibit the high-symmetry P4 structure. Instead the structure obtained for the QPDC ligand corresponds to the P2

structure also seen for MOF-2 (see Fig. S3, supporting information). The ligand PPDC, pentaphenyldicarboxylic acid, with a length of 2.5 nm, to our knowledge, is among the longest ligands which have so far been used successfully for a MOF synthesis, only in the very recent work by Deng et al.<sup>30</sup> this length has been exceeded. A detailed analysis of the diffraction data allowed us to propose the structures shown in Fig. 1. This novel isorecticular series of MOFs, hereafter termed SURMOF-2, also consists of pw-planes, which – in contrast to MOF-2 – are stacked directly on-top of each other. This absence of a lateral shift when stacking the pw-planes yields 1d-pores of quadratic cross section with a diagonal up to 4 nm (see Fig. 2). Importantly, for the SURMOF-2 series, interpenetration is absent. For many known isorecticular MOF series, the formation of larger and larger pores is limited by this phenomenon: if the pores become too large, a second or even a third 3d-lattice will be formed inside the first lattice yielding interpenetrated networks, which exhibit the expected larger lattice constant but with rather small pore sizes<sup>31</sup>, the hosting of NPs thus becomes impossible. For SURMOF-2, like for other MOF-structures with the appropriate topology (non self-complementary nets, see Ref. 30 and references cited there) the presence of 1d-pores of quadratic cross section is not compatible with a second, interwoven network and, as a result, interpenetration is suppressed.

Although the solubility of the long dicarboxylic acids TPDC, QPDC and PPDC, (see Fig. 1) used as ligands for the SURMOF-2 fabrication is fairly small, we encountered no problems in the LPE process. This can be understood by considering that already small concentrations of dicarboxylic acids are sufficient for the formation of a single monolayer on the substrate, the elementary step of the LPE synthesis process<sup>32</sup>. Even with the longest dicarboxylic acid available to us, PPDC, growth occurred in a straightforward fashion and optimization of the growth process was not necessary.

**Theory.** The P4 structures proposed for the SURMOF-2 series, except for the 2,6-NDC ligand, differ markedly from the bulk MOF-2 structures obtained from conventional solvothermal synthesis<sup>24,27,28</sup>. To understand this unexpected difference, and in particular the absence of relative shifts between the pw-planes in the proposed SURMOF-2 structure, we performed extensive quantum chemical calculations, employing an approximate variant of density-functional theory (DFT), London dispersion-corrected self-consistent charge density-functional based tight-binding (DFTB)<sup>33–35</sup>. We studied a periodic model of MOF-2 as well as different SURMOF derivatives.

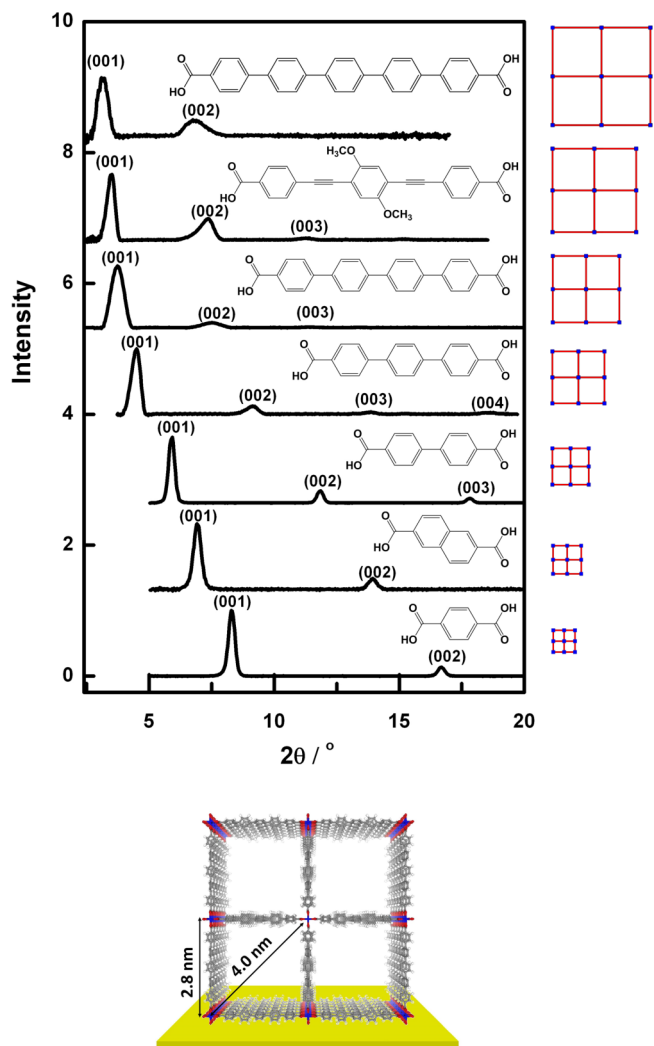


**Figure 2** | Out of plane XRD data of Cu-BDC, Cu-2,6-NDC, Cu-BPDC, Cu-TPDC, Cu-QPDC, Cu-P(EP)<sub>2</sub>DC and Cu-PPDC (upper left), schematic representation (upper right) and proposed structures of SURMOF-2 analogues (lower panel). All the SURMOF-2 are grown on -COOH terminated SAM surface using the LPE method.

Periodic structure DFTB calculations (Fig. S1) confirmed that the P2/m structure, proposed by Yaghi et al. for the bulk MOF-2 material<sup>24</sup>, is indeed the energetically most favorable configuration for MOF-2, while the C2/m structure, that has also been reported for bulk MOF-2<sup>27,28</sup> is slightly higher in energy (41 meV per formula

**Table 1** | Stacking energy and geometries of P4 SURMOF-2 derivatives

	Symmetry	a = c	b	Stacking Energy*
<b>Cu<sub>2</sub>(BDC)<sub>2</sub></b>	C2	11.19	5.0	-0.76
<b>Cu<sub>2</sub>(BDC)<sub>2</sub></b>	P2	11.19	5.4	-0.8
<b>Cu<sub>2</sub>(BDC)<sub>2</sub></b>	P4	11.19	5.8	-0.59
<b>Cu<sub>2</sub>(BDC)<sub>2</sub></b>	P2	13.35	5.6	-0.4
<b>Cu<sub>2</sub>(BPDC)<sub>2</sub></b>	P4	15.49	5.9	-0.68
<b>Cu<sub>2</sub>(TPDC)<sub>2</sub></b>	P4	19.84	5.9	-0.91
<b>Cu<sub>2</sub>(QPDC)<sub>2</sub></b>	P4	24.24	5.9	-1.21
<b>Cu<sub>2</sub>(P(EP)<sub>2</sub>DC)<sub>2</sub></b>	P4	25.12	5.2	-1.73
<b>Cu<sub>2</sub>(PPDC)<sub>2</sub></b>	P4	28.59	5.9	-1.45

\*Stacking energies (DFTB level, in eV) of SURMOFs. The energies were calculated within periodic boundary conditions and are given per formula unit.

unit, see Table 1). The optimum interlayer distance between the pw-planes in the P4 structure is 5.8 Å, in very good agreement with the experimental value of 5.6 Å (as obtained from the in-plane XRD-data, see Fig. S2). It is important to note that at that distance the linkers cannot remain in rectangular position as in MOF-2, but are twisted in order to avoid steric hindrance and to optimize linker-linker interactions.

The P4/mmm structure, as proposed for SURMOF-2, is less stable by 200 meV per formula unit as compared to the P2/m configuration. Although the crystal energy for the P4 stacking is substantially smaller than that for the P2 packing, simulated annealing (DFTB model using Born-Oppenheimer Molecular Dynamics) carried out at 300 K for 10 ps demonstrated that the P4/mmm structure corresponds to a local minimum. This observation is confirmed by the calculation of the stacking energy of MOF-2, where a shifting of the layers is simulated along the P2-P4-C2 path (Figure 3). On the basis of these calculations, we thus propose that SURMOF-2 adopts the metastable P4 structure.

In Table 1, the interlayer interaction energies are summarized. They range from 590 meV per formula unit with respect to fully dissociated MOF-2 layers for Cu<sub>2</sub>(bdc)<sub>2</sub> and successively increase for longer linkers of the same type, reaching 1.45 eV per formula unit for Cu<sub>2</sub>(ppdc)<sub>2</sub>, indicating that the linkers play an important role in the overall stabilization of SURMOF-2 with large pore sizes. Even stronger interlayer interactions are found for different linker topologies (PPDC). Additional calculations carried out reveal that the presence of ligands like DMF (dimethylformamide) or water destabilizes the P4 structure by inducing shifts between the pw-planes. A detailed computational analysis of the role of the individual building blocks of SURMOF-2 for the crystal growth and stabilization as well as the role of solvent molecules will be published elsewhere.

## Discussion

The flat, well-defined organic surfaces used as the templating (or nucleating) substrate in the LPE growth process provide an excellent explanation for why SURMOF-2 grows with the highly symmetrical P4 structure instead of adopting the energetically more favorable, low symmetry bulk P2 (or C2) symmetry<sup>32,36</sup>. The carboxylic acid groups exposed on the surface force the first layer of deposited Cu-dimers into a coplanar arrangement, which is not compatible with the bulk P2 (or C2) structure, but, rather, nucleates the P4 packing. In turn, the carboxylate-groups in the first layer of deposited dicarboxylic

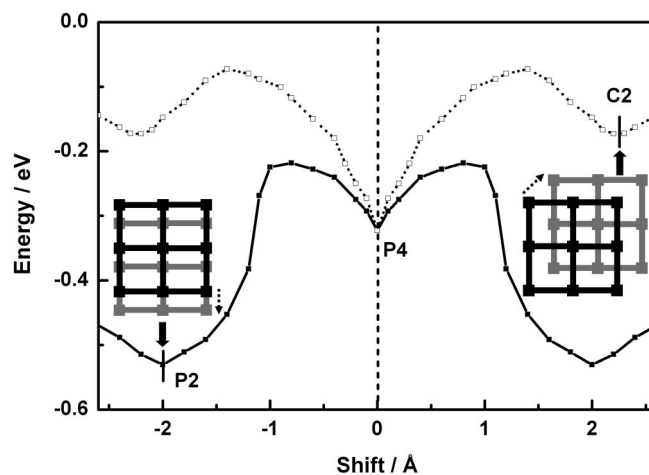


**Figure 3** | Energy for the relative shift of each layer in two different directions: horizontal (P4 to P2) and diagonal (P4 to C2) at a fixed interlayer distance of 5.6 Å. Structures have been partially optimized and energies are given per formula unit with respect to fully dissociated planes.





acids provide the same constraints for the next layer (see Fig. 1). As a result of the layer-by-layer method employed for further SURMOF-2 growth, the same boundary conditions apply for all subsequent layers. The organic surface thus acts as a seed structure to yield the metastable P4 packing, not an unusual motif in epitaxial growth<sup>37</sup>.

Furthermore, the calculations allow us to predict that it will be possible to grow SURMOF structures with even larger linker molecules as used here. The  $\pi$  stacking will further stabilize the P4 symmetry as the interaction energy per formula unit is more and more dominated by the linkers (Table 1). At present, we cannot predict the maximum possible size of the pores, one may speculate that by adding additional functionalities to the linkers the linker-linker interaction may be sufficiently large to exceed 10 nm  $\times$  10 nm and thus reach a size regime which is of interest for the realization of plasmonic structures by embedding metal nanoparticles<sup>6</sup>.

## Methods

**Computational details.** All structures were created using a preliminary version of our topological framework creator software, which allows the creation of topological network models in terms of secondary building units and their replacement by individual molecules to create the coordinates of virtually any framework material. The generated starting coordinates, including their corresponding lattice parameters, have been hierarchically fully optimized using the Universal Force Field (UFF)<sup>38</sup>, followed by the dispersion-corrected self-consistent-charge density-functional based tight-binding (DFTB) method<sup>33–35,39,40</sup> that we have recently validated against experimental structures of HKUST-1, MOF-5, MOF-177, DUT-6 and MIL-53(Al), as well as for their performance to compute the adsorption of water and carbon monoxide<sup>34</sup>. For all calculations, we employed the deMonNano software<sup>41</sup>. We have chosen periodic boundary conditions for all calculations, and the repeated slab method has been employed to compute the properties of the single layers in order to evaluate the stacking energy. A conjugate-gradient scheme was employed for geometry optimization of atomic coordinates and cell dimensions. The atomic force tolerance was set to  $3 \times 10^{-4}$  eV/Å.

The confined conditions at the SURMOF-substrate interface was modeled by fixing the corresponding coordinate in the computer simulations. All calculated structures have been substantiated by simulated annealing calculations, where a Born-Oppenheimer Molecular Dynamics trajectory at 300 K has been computed for 10 ps without geometry constraints. All structures remained in P4 topology.

**Experimental methods.** The SURMOF-2 samples were grown on Au substrates (100-nm Au/5-nm Ti deposited on Si wafers) using a high-throughput approach, spray method<sup>42</sup>. The gold substrates were functionalized by self-assembled monolayers, SAMs, of 16-mercaptohexadecanoic acid (MHDA). These substrates were mounted on a sample holder and subsequently sprayed with a 1 mM solution of  $\text{Cu}_2(\text{CH}_3\text{COO})_4 \cdot \text{H}_2\text{O}$  in ethanol and an ethanolic solution of SURMOF-2 organic linkers (0.1 mM of BDC, 2,6-NDC, BPDC and saturated solutions of TPDC, QPDC, PPDC, P(EP)<sub>2</sub>DC) at room temperature. The number of spray cycles employed was different for different linkers (PPDC: 90, TPDC: 80, QPDC: 50 and P(EP)<sub>2</sub>DC: 50, BDC, 2,6-NDC and BPDC: all 20). After synthesis all samples were characterized with X-ray diffraction (XRD). The solvothermal synthesis condition for (Cu-QPDC) MOF-2 were as those reported for (Cu, BDC) MOF-2<sup>24</sup>. Ethanol and DMF were used as solvents.

1. Wang, B., Cote, A. P., Furukawa, H., O'Keeffe, M. & Yaghi, O. M. Colossal cages in zeolitic imidazolate frameworks as selective carbon dioxide reservoirs. *Nature* **453** (7192), 207–U206 (2008).
2. Lauren, E. Kreno *et al.* Metal-Organic Framework Materials as Chemical Sensors. *Chemical Reviews* **112**, 1105–1124 (2012).
3. Dragasser, A. *et al.* Redox mediation enabled by immobilised centres in the pores of a metal-organic framework grown by liquid phase epitaxy. *Chemical Communications* **48** (5), 663–665 (2012).
4. Lykourinou, V. *et al.* Immobilization of MP-11 into a Mesoporous Metal-Organic Framework, MP-11@mesoMOF: A New Platform for Enzymatic Catalysis. *J. Am. Chem. Soc.* **133** (27), 10382–10385 (2011).
5. Horcajada, P. *et al.* Flexible porous metal-organic frameworks for a controlled drug delivery. *J. Am. Chem. Soc.* **130** (21), 6774–6780 (2008).
6. Hurd, J. A. *et al.* Anhydrous proton conduction at 150 degrees C in a crystalline metal-organic framework. *Nat. Chem.* **1** (9), 705–710 (2009).
7. Kreno, L. E., Hupp, J. T. & Van Duyne, R. P. Metal-Organic Framework Thin Film for Enhanced Localized Surface Plasmon Resonance Gas Sensing. *Analytical Chemistry* **82** (19), 8042–8046 (2010).
8. Lu, G. *et al.* Fabrication of Metal-Organic Framework-Containing Silica-Colloidal Crystals for Vapor Sensing. *Advanced Materials* **23** (38), 4449–4452 (2011).
9. Lu, G. & Hupp, J. T. Metal-Organic Frameworks as Sensors: A ZIF-8 Based Fabry-Perot Device as a Selective Sensor for Chemical Vapors and Gases. *J. Am. Chem. Soc.* **132** (23), 7832–7833 (2010).

10. Allendorf, M. D., Schwartzberg, A., Stavila, V. & Talin, A. A. A Roadmap to Implementing Metal-Organic Frameworks in Electronic Devices: Challenges and Critical Directions. *Chemistry-a European Journal* **17** (41), 11372–11388 (2011).
11. Liu, B. *et al.* Enantiopure Metal-Organic Framework Thin Films: Oriented SURMOF Growth and Enantioselective Adsorption. *Angewandte Chemie-International Edition* **51**, 817–810 (2012).
12. Sadakiyo, M., Yamada, T. & Kitagawa, H. Rational Designs for Highly Proton-Conductive Metal-Organic Frameworks. *J. Am. Chem. Soc.* **131** (29), 9906–9907 (2009).
13. Eddaoudi, M. *et al.* Systematic design of pore size and functionality in isorecticular MOFs and their application in methane storage. *Science* **295** (5554), 469–472 (2002).
14. Ishida, T., Nagaoka, M., Akita, T. & Haruta, M. Deposition of Gold Clusters on Porous Coordination Polymers by Solid Grinding and Their Catalytic Activity in Aerobic Oxidation of Alcohols. *Chemistry-a European Journal* **14** (28), 8456–8460 (2008).
15. Esken, D., Turner, S., Lebedev, O. I., Van Tendeloo, G. & Fischer, R. A. Au@ZIFs: Stabilization and Encapsulation of Cavity-Size Matching Gold Clusters inside Functionalized Zeolite Imidazolate Frameworks, ZIFs. *Chemistry of Materials* **22** (23), 6393–6401 (2010).
16. Lohe, M. R. *et al.* Heating and separation using nanomagnet-functionalized metal-organic frameworks. *Chemical Communications* **47** (11), 3075–3077 (2011).
17. Lu, G. *et al.* Imparting functionality to a metal-organic framework material by controlled nanoparticle encapsulation. *Nat. Chem.* **4** (4), 310–316 (2012).
18. Gliemann, H. & Wöll, C. Epitaxially grown metalorganic frameworks. *Materials Today* **15** (3), 110–116 (2012).
19. Shekhah, O. *et al.* Step-by-step route for the synthesis of metal-organic frameworks. *J. Am. Chem. Soc.* **129** (49), 15118–15119 (2007).
20. Furukawa, S. *et al.* A block PCP crystal: anisotropic hybridization of porous coordination polymers by face-selective epitaxial growth. *Chemical Communications* **34**, 5097–5099 (2009).
21. Shekhah, O. *et al.* MOF-on-MOF heteroepitaxy: perfectly oriented [Zn(2)(ndc)(2)(dabco)](n) grown on [Cu(2)(ndc)(2)(dabco)](n) thin films. *Dalton Transactions* **40** (18), 4954–4958 (2011).
22. Shekhah, O. *et al.* Controlling interpenetration in metal-organic frameworks by liquid-phase epitaxy. *Nature Materials* **8** (6), 481–484 (2009).
23. Zacher, D. *et al.* Liquid-Phase Epitaxy of Multicomponent Layer-Based Porous Coordination Polymer Thin Films of [M(L)(P)0.5] Type: Importance of Deposition Sequence on the Oriented Growth. *Chemistry-a European Journal* **17** (5), 1448–1455 (2011).
24. Li, H., Eddaoudi, M., Groy, T. L. & Yaghi, O. M. Establishing microporosity in open metal-organic frameworks: Gas sorption isotherms for Zn(BDC) (BDC = 1,4-benzenedicarboxylate). *J. Am. Chem. Soc.* **120** (33), 8571–8572 (1998).
25. Mueller, U. *et al.* Metal-organic frameworks - prospective industrial applications. *Journal of Materials Chemistry* **16** (7), 626–636 (2006).
26. Shekhah, O., Wang, H., Zacher, D., Fischer, R. A. & Wöll, C. Growth Mechanism of Metal-Organic Frameworks: Insights into the Nucleation by Employing a Step-by-Step Route. *Angewandte Chemie-International Edition* **48** (27), 5038–5041 (2009).
27. Carson, C. G. *et al.* Synthesis and Structure Characterization of Copper Terephthalate Metal-Organic Frameworks. *European Journal of Inorganic Chemistry* (16), 2338–2343 (2009).
28. Clausen, H. F., Poulsen, R. D., Bond, A. D., Chevallier, M. A. S. & Iversen, B. B. Solvothermal synthesis of new metal organic framework structures in the zinc-terephthalic acid-dimethyl formamide system. *Journal of Solid State Chemistry* **178** (11), 3342–3351 (2005).
29. Arslan, H. K. *et al.* Intercalation in Layered Metal-Organic Frameworks: Reversible Inclusion of an Extended pi-System. *J. Am. Chem. Soc.* **133** (21), 8158–8161 (2011).
30. Deng, H. *et al.* Large-Pore Apertures in a Series of Metal-Organic Frameworks. *Science* **336**, 1018 (2012).
31. Yaghi, O. M. A tale of two entanglements. *Nature Materials* **6** (2), 92–93 (2007).
32. Shekhah, O., Liu, J., Fischer, R. A. & Wöll, C. MOF thin films: existing and future applications. *Chemical Society Reviews* **40** (2), 1081–1106 (2011).
33. Elstner, M. *et al.* Self-consistent-charge density-functional tight-binding method for simulations of complex materials properties. *Physical Review B* **58** (11), 7260–7268 (1998).
34. Lukose, B. *et al.* Structural properties of metal-organic frameworks within the density-functional based tight-binding method. *Physica Status Solidi B-Basic Solid State Physics* **249** (2), 335–342 (2012).
35. Zhechkov, L., Heine, T., Patchkovskii, S., Seifert, G. & Duarte, H. A. An efficient a posteriori treatment for dispersion interaction in density-functional-based tight binding. *Journal of Chemical Theory and Computation* **1** (5), 841–847 (2005).
36. Zacher, D., Schmid, R., Wöll, C. & Fischer, R. A. Surface Chemistry of Metal-Organic Frameworks at the Liquid-Solid Interface. *Angewandte Chemie-International Edition* **50** (1), 176–199 (2011).
37. Prinz, G. A. Stabilization of bcc Co via Epitaxial Growth on GaAs. *Physical Review Letters* **54** (10), 1051–1054 (1985).
38. Rappe, A. K., Casewit, C. J., Colwell, K. S., Goddard, W. A. & Skiff, W. M. UFF, a full periodic table force field for molecular mechanics and molecular dynamics simulations. *J. Am. Chem. Soc.* **114** (25), 10024–10035 (1992).
39. Seifert, G., Porezag, D. & Frauenheim, T. Calculations of molecules, clusters, and solids with a simplified LCAO-DFT-LDA scheme. *International Journal of Quantum Chemistry* **58** (2), 185–192 (1996).



40. Oliveira, A. F., Seifert, G., Heine, T. & Duarte, H. A. Density-Functional Based Tight-Binding: an Approximate DFT Method. *Journal of the Brazilian Chemical Society* **20** (7), 1193–1205 (2009).
41. deMonNano v. 2009 (*Bremen, 2009*).
42. Arslan, H. K. *et al.* High-Throughput Fabrication of Uniform and Homogenous MOF Coatings. *Advanced Functional Materials* **21** (22), 4228–4231 (2011).

## Acknowledgements

We thank Ms. Hülsmann, Bielefeld University, for the preparation of P(EP)<sub>2</sub>DC. Financial support by Deutsche Forschungsgemeinschaft (DFG) within the Priority Program Metal-Organic Frameworks (SPP 1362) is gratefully acknowledged. T.H. acknowledges financial support by the European Research Council (GA ERC-StG-256962 C3ENV).

## Author contributions

J.L., O.S., H.K.A. prepared the SURMOFs investigated in this study. S.B., S.G., X.F. and K.M. synthesized the organothiols used to fabricate the SURMOFs. B.L., I.-B. M. and T.H. carried

out the calculations. Data analysis was carried out by P.W., H.G. and C.W. The work was directed by A.G., K.M., T.H. and C.W. All authors contributed equally in writing the manuscript.

## Additional information

**Supplementary information** accompanies this paper at <http://www.nature.com/scientificreports>

**Competing financial interests:** The authors declare no competing financial interests.

**License:** This work is licensed under a Creative Commons Attribution-NonCommercial-NoDerivs 3.0 Unported License. To view a copy of this license, visit <http://creativecommons.org/licenses/by-nc-nd/3.0/>

**How to cite this article:** Liu, J. *et al.* A novel series of isorecticular metal organic frameworks: realizing metastable structures by liquid phase epitaxy. *Sci. Rep.* **2**, 921; DOI:10.1038/srep00921 (2012).